physical observables of the sensor file into geophysical measurements of interest to end users. Geophysical algorithms also make corrections for atmospheric and surface effects which influence the desired geophysical measurements.

The altimeter geophysical algorithms provide corrections for refraction caused by the ionosphere and by air and water in the atmosphere and for modeled ocean surface effects such as tides (ocean and solid earth), atmospheric pressure loading, water density (salinity), and the geoid. In addition, one algorithm converts radar backscatter to wind speed and another replaces the medium-accuracy (50 m) location information obtained from the SDR (by way of the sensor file) with more precise orbit information (2 to 3 m) calculated from the best available tracking data.

The SASS geophysical algorithms convert radar backscatter measurements to wind vectors by combining measurements made in orthogonal directions and applying one of several models to the measurements. Because of the form of the functional relationship between wind vectors and backscatter measurements, the wind vector algorithms yield multiple solutions called "aliases." Work on an algorithm to select the correct solution from the aliases, typically four in number, is still in a preliminary stage. Currently available data products contain up to four wind solutions at each measurement point. A planetary boundary layer model is also planned for inclusion in the SASS geophysical algorithms so that winds will be reported both as friction velocity (u^*) and as winds at a height of 19.5 m. Also planned for future inclusion is a set of algorithms that will use microwave brightness measurements from SMMR to correct the SASS backscatter measurements for the effect of atmospheric attenuation. This is currently thought to be a negligible effect, except in heavy rain cells.

The SMMR geophysical algorithms are derived from models of ocean surface emissivity and atmospheric emission and absorption. These models are effectively inverted to derive estimates of ocean surface temperature, wind speed, and atmospheric water content (liquid and vapor). In addition, an estimate of the integrated water column is converted to a refractive path length correction for the altimeter.

Two catalogs of the Seasat data, the MSDR catalog and the general catalog, are available to provide convenient access to data of specific interest among the thousands of reels of tape. The Seasat data base consists of a number of large, time-ordered data sets on magnetic tape, specifically: the MSDR, SDR, IGDR sensor files, and IGDR geophysical files. Only the MSDR contains all the available data; the others contain subsets.

The MSDR catalog is a detailed summary of all the MSDR tapes and can be searched for data satisfying any desired combination of geography, instrument mode, and time span. Search results include tape reel numbers and other access information and specific time intervals within each tape reel which contain data satisfying all user-specified criteria. The general catalog is essentially a cross-reference between time and tape reel number, for all types of data tapes.

Both catalogs are on-line and can be searched interactively by users with remote terminals. One would begin a typical search by specifying a geographical region, time span, and sensor or sensors of interest and executing a search in the MSDR catalog. The resulting times can then be checked in the general catalog to determine the availability of data processed to any of the other forms.

J. W. BROWN, G. C. CLEVEN
J. C. KLOSE, D. B. LAME
C. A. YAMARONE

Jet Propulsion Laboratory, California Institute of Technology, Pasadena 91103

References

1. The research described in this report was carried out by the Jet Propulsion Laboratory, California Institute of Technology, under NASA contract NAS7-100.

20 April 1979

Surface Observations for the Evaluation of Geophysical Measurements from Seasat

Abstract. *The surface observations used in the initial assessment of Seasat are discussed with emphasis on their ability to describe the synoptic-scale winds over the ocean.*

We made the initial assessment of the capabilities of Seasat by comparing subsets of the satellite data against conventional measurements, both in situ and remote. These data are sometimes referred to as surface truth data but can be more accurately described as surface observations. These observations were used for direct comparison with Seasat-derived values at fixed locations as well as for input to analyzed fields of pressure, wind, air and sea temperatures, and surface dew point.

The principal source of conventional measurements was a series of special observations taken in August and September 1978 during an intensive data-gathering effort in the northwest Pacific termed the Gulf of Alaska Seasat Experiment (GOASEX). Measurement platforms consisted of National Oceanic and Atmospheric Administration (NOAA) data buoys, the NOAA research vessel *Oceanographer*, and two Canadian weather ships, *Quadra* and *Vancouver*, which were stationed alternately at ocean station PAPA (50°N, 145°W). In addition to the standard surface and upper-air weather observations, the investigators on the ships took special surface wind and wave measurements that began 10 minutes before and ended 10 minutes after the arrival of the satellite. Buoys reported standard observations hourly. Four aircraft (two National Aeronautics and Space Administration, one U.S. Navy, and one Canadian) flew over either ships or buoys for selected orbits, taking remotely sensed data on surface and flight-level winds, air and sea temperatures, and ocean waves. A less reliable source of measurement, but one that was essential to the construction of fields, was the network of weather observations from ships reporting through the World Weather Watch and the Fleet Numerical Weather Central at 0000, 0600, 1200, and 1800 G.M.T.

Visible and infrared satellite imagery from the Geostationary Operational Environmental Satellite (GOES) and NOAA-5 weather satellites, and from the Defense Meteorological Satellite Program, provided additional sources of detailed analyses of cloud cover and precipitation.

In general, the reliability of observations ranged from excellent to fair. The most reliable observations were those from *Oceanographer* and the weather ships which reported at satellite overpass times. The least reliable were observations from merchant ships reporting visual observations at other than overpass times. For surface winds, the accuracy of measurement has been shown to be a function of the type of ship making the report (*1*). Weather ships gave the most accurate measurements, and less accurate measurements were obtained on ships with anemometers at a known height. Ships without anemometers, which reported wind speeds based on the Beaufort scale, gave the least accurate measurements.

One reason for large errors in surface wind reports from ships was that the conventional 2-minute average in standard weather observations was insufficient to describe the mean wind accurately. This is illustrated in Fig. 1, which shows a wind record made by *Quadra* at ocean station PAPA. The recorded wind speed fluctuated from 30 knots (15.4 m/sec) to 50 knots during the 23-minute period. The mean wind speed was 39.3 knots, but almost all 2-minute segments yielded wind speeds different from this and the wind speeds of a few segments differed by as much as 8 knots. Comparisons of Seasat-derived surface winds were thus stratified by types of platforms.

Fields of sea level pressure (SLP), surface winds, cloud cover and precipitation, air and sea temperatures, and dew point were manually produced for the times of selected orbits over the Gulf of Alaska. We generated these fields by using Weather Service and Fleet Numerical Weather Central operational field products as an initial guess field. We refined the guess field by using GOES and NOAA-5 imagery and incorporating the special observations acquired by the ship and buoy network. A monthly mean sea-surface temperature chart for September 1978, from the National Marine Fisheries Service, was also used in the evaluation.

The wind fields were developed from SLP and ancillary fields by a planetary boundary layer (PBL) model, and by a streamline-isotach or kinematic analysis based upon direct anemometer measurements. We derived PBL model winds from surface pressure measurements by assuming vertical coherency in the pressure field, so that the free-stream (geostrophic) winds were determined from the surface pressure gradients. The wind constituted the upper boundary condition for the two-layer (PBL) model which related these gradient winds to surface wind vectors. The modeled wind fields were compared to the observed winds, and discrepancies were used to reanalyze the surface pressure fields. The final modeled wind fields were the result of a tuned pressure analysis, having second and sometimes third iterations.

The kinematic analysis gave primary weight to the wind observations, although they were few in number, with secondary consideration given to pressure gradient. By imposing continuity considerations, an entire sequence of wind analyses at discrete times in a specific storm was assembled into a credible three-dimensional series. In the analysis, wind observations from ships with anemometers at known heights were reduced to an effective wind at a height of 19.5 m (64 feet) and to neutral stability. We corrected the Beaufort estimates to equivalent 19.5-m wind speeds, using the scale described by Cardone (*2*).

Subjectively derived confidence estimates were provided for squares 2.5° in latitude and 2.5° in longitude for both techniques, based on the data density and the type of reporting platform. The two types of wind fields were plotted and compared. The extent of agreement between the two was used as a further confidence indicator in the validation of Seasat-derived winds.

We constructed the cloud cover and precipitation analyses, using GOES and NOAA-5 visible and enhanced infrared imagery and ship and buoy weather reports. In the cloud analysis we used GOES infrared imagery. This analysis was examined in light of GOES visible and enhanced infrared imagery to locate clouds at subfreezing temperatures, cumulonimbus towers, and cirrus cover without precipitating clouds underneath. All available ship and buoy reports were plotted and compared for consistency, and a final analysis of clouds and precipitation was constructed. These analyses delineated areas of cloud cover without precipitation and areas of possible, probable, and almost certain precipitation.

An example of validation comparisons for the Seasat-A scatterometer system (SASS) performance are shown in Table 1 for individual observations and for interpolations from fields produced by two

Table 1. Results of a preliminary comparison of SASS-derived winds (combined vertical and horizontal polarization data) with winds specified by several types of platforms and by two types of analyzed fields.

Surface data type	Wind speed		Wind direction		*N*
	Mean error (m/sec)	Standard deviation	Mean error (degrees)	Standard deviation	
Buoys and weather ships	1.8	0.9	2.3	16.2	22
Transient ships	2.7	2.7	2.2	22.3	63
Kinematic analysis (orbit 1140, all data)	2.9	2.5	−3.7	16.4	214
Modeled winds (orbit 1140, all data)	5.1	2.5	0.6	18.8	211
Kinematic analysis (orbit 1298, all data)	2.0	1.8	−0.1	22.2	156
Modeled winds (orbit 1298, all data)	1.2	2.3	−4.2	28.2	158

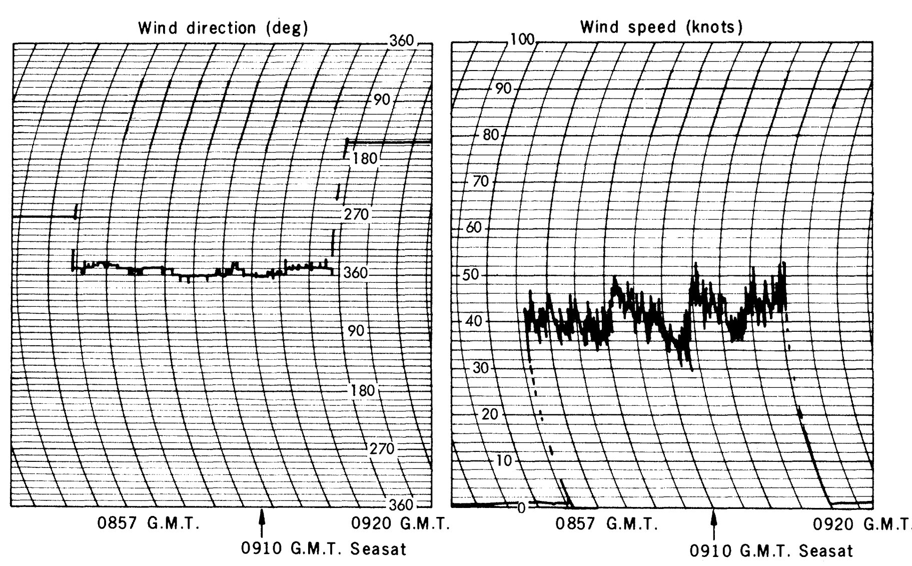

Fig. 1. Anemometer record of strong gusty winds from the weather ship *Quadra* at ocean weather station PAPA: orbit 1135, 14 September 1978, 0857 to 0920 G.M.T.; ship location, 260°; ship speed, 2 knots.

methods. Table 1 illustrates the sensitivity of the verification statistics to the type of comparison data used for evaluation. The statistics for buoys, weather ships, and transient ships (those with and without anemometers have been combined) were based upon comparisons of several revolutions. The statistics for fields are shown for two revolutions (1140, which contained high winds, and revolution 1298, which was characterized by low winds). The statistics showed that the lowest errors (standard deviations) occurred for the buoys and weather ships where averaging periods ranged from 8.5 to 20 minutes or longer, and the greatest errors occurred with transient ships where a 2-minute averaging period was used. It appeared that the stratification seen in the statistics of these comparisons was attributable largely to the lower accuracy of the 2-minute surface wind measurements from transient ships and their subsequent effect on the fields.

J. C. WILKERSON
National Environmental Satellite Service, National Oceanic and Atmospheric Administration, Camp Springs, Maryland 20023
R. A. BROWN
University of Washington, Seattle 98109
V. J. CARDONE
Oceanweather, Inc., White Plains, New York 10601
R. E. COONS, A. A. LOOMIS
Jet Propulsion Laboratory, California Institute of Technology, Pasadena 91103
J. E. OVERLAND
Pacific Marine Environmental Laboratory, National Oceanic and Atmospheric Administration, Seattle, Washington 98109
S. PETEHERYCH
Atmospheric Environmental Service, Downsview, Ontario, Canada M3H 5T4
W. J. PIERSON
City University of New York, New York 10031
P. M. WOICESHYN
Jet Propulsion Laboratory
M. G. WURTELE
University of California, Los Angeles 90024

References and Notes

1. V. J. Cardone *et al.*, *NASA Contract Rep. 1-7487* (1976).
2. V. J. Cardone, "Specification of wind distribution in the marine boundary layer for wave forecasting" (Publication AD-702490 GSI-TR-69-1, Geophysical Sciences Laboratory, New York University, New York, 1969).
3. A portion of the work described in this report represents results of one phase of work conducted at the Jet Propulsion Laboratory, California Institute of Technology, under NASA contract NAS7-100.

20 April 1979

Seasat Altimeter Calibration: Initial Results

Abstract. *Preliminary analysis of radar altimeter data indicates that the instrument has met its specifications for measuring spacecraft height above the ocean surface (± 10 centimeters) and significant wave height (± 0.5 meter). There is ample evidence that the radar altimeter, having undergone development through three earth orbit missions [Skylab, Geodynamics Experimental Ocean Satellite 3 (GEOS-3), and Seasat], has reached a level of precision that now makes possible its use for important quantitative oceanographic investigations and practical applications.*

The objective of the Seasat altimeter calibration is to obtain an accurate value of the precision of the altimeter height measurement (*1*), the bias in the height measurement, the bias in the data time tag, and the accuracy of the altimeter in measuring significant wave heights (SWH) and surface wind speeds (*2*). The data required to calibrate the altimeter were obtained during September 1978 in two different regions, the Gulf of Alaska and the Bermuda Calibration Area. The Gulf of Alaska Seasat Experiment data set was used as the primary data source for calibrating SWH and the radar backscatter coefficient, σ^0. For the height bias determination, the spacecraft was maneuvered so that, beginning 10 September 1978, the orbit passed over the Bermuda laser tracking station from northeast to southwest once every 3 days. During the next month the Bermuda laser was successful in tracking the spacecraft during four overflights whose ground tracks passed within 5 km of the laser site. The precision of the laser tracking data was ± 8 cm during each pass.

The altimetry data used for the calibration are the raw measurements corrected for instrument, atmospheric, and geophysical effects. Consequently, determination of the altimeter height bias and the accuracy of SWH and σ^0 measurements requires an associated validation of the correction algorithms. The basic height calibration geometry is shown in Fig. 1 (*3*). By assuming a high-elevation pass with continuous laser and altimeter ranging, one can use the measurements directly over the tracking station for bias estimation by equating the altimeter measurement, extrapolated to the ellipsoid, to the extrapolated laser measurement (*4*). Equating the two measurements (Fig. 1) leads to the following relation (*5*):

$$h_a - b + h_t + \delta h + h_g(a) = h_g(s) + h_m + R$$

If all other terms have been evaluated, Eq. 1 can be used to determine b. The terms after the equal sign yield the calculated spacecraft height above the ellipsoid as determined in most orbit determination programs. The terms $h_a - b$ are based on the altimeter measurement, which must be related to the ellipsoid through a tide model (*6*) and a geoid model (*7*). An ionospheric and tropospheric correction model also is required (*8*). Using Eq. 1, one can calculate b (even though the satellite may not pass directly over the laser) if allowances are made for changes in the geoid between the altimeter footprint and the laser site.

Since the altimeter cannot track over land to the accuracy required for the bias determination and the laser cannot track directly overhead because of mount constraints, two special approaches were

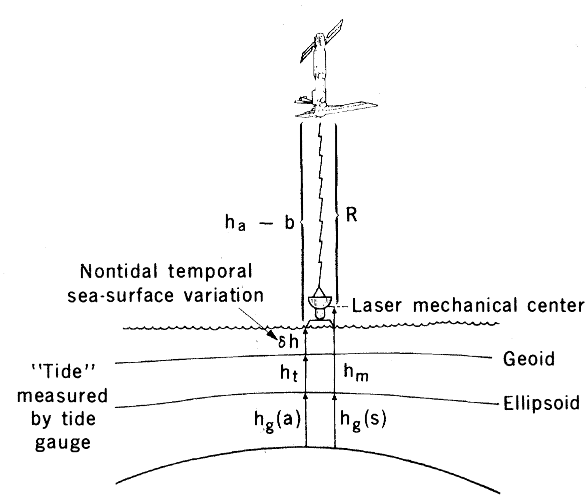

Fig. 1. Calibration geometry based on the use of the overhead pass.